

SEDIMENTATION OF PARTICLES IN POLYMER SOLUTIONS

Yaoqi Joe Liu and Daniel D. Joseph
Department of Aerospace Engineering and Mechanics
University of Minnesota, Minneapolis, MN 55455, USA
(June, 1992)

ABSTRACT

In this paper, we present detailed and systematic experimental results on the sedimentation of solid particles in aqueous solutions of polyox and polyacrylamide. The tilt angles of long cylinders falling in these viscoelastic liquids were measured. The effects of particle length, particle weight, particle shape, liquid properties and liquid temperature were determined. In these experiments, the cylinders fall under gravity in a two-dimensional bed. No matter how or where they are released they will center themselves between the close walls and fall steadily in a configuration in which the axis of the cylinder is at a fixed angle of tilt with the horizontal. A discussion of the tilt angle may be framed in terms of competition between viscous effects, viscoelastic effects and inertia. When inertia is large the particles settle with their broadside perpendicular to the direction of fall. When inertia is small viscoelasticity dominates and the particles settle with their broadside parallel to the direction of fall. The tilt angle varies continuously from 90° when viscoelasticity dominates to 0° when inertia dominates. The balance between inertia and viscoelasticity was controlled by systematic variation of the weight of the particles, the concentration of polyox in water and of the temperature of the solution. Particles will turn broadside-on when the inertia forces are larger than viscous and viscoelastic forces. This orientation occurred when the Reynolds number was greater than some number not much greater than one in any case, and less than 0.1 in Newtonian liquids and very dilute solutions. The appearance of a tilt angle, however, appears to be most strongly correlated with values of a viscoelastic Mach number $M=U/c$ where U is the terminal velocity and c is the shear wave speed measured with the shear wave speed meter (Joseph, [1990]). Strong departure of the tilt angle from $\theta=90^\circ$ begins at about $M=1$ and ends with $\theta=0^\circ$ when $1<M<4$. The dynamics which controls this orientation transition is provisionally interpreted as a change of type. We also report measurements of the parameters which control a newly observed non-Newtonian flow phenomenon, the anomalous rolling of a sphere in a viscoelastic fluid down an inclined wall (Joseph, Nelson, Hu and Liu [1992]): a sphere falling close to an inclined wall rotates as if rolling down the wall in the intuitive way in a viscous liquid, but rotates as if rolling up the wall against intuition in a viscoelastic liquid. The angular speed of the anomalous rolling spheres actually increases as the angle of inclination of the wall and fall velocity increases.

1. INTRODUCTION

Michele, Pätzold and Donis [1977] have noted that small spheres ($\sim 70\mu\text{m}$) in an oscillating liquid sheared by the back and forth motion of parallel plates, or cone and plates (Highgate [1966], Highgate and Whorlow [1969], Petit and Noetinger [1988]) align in the direction of shear when the liquid is viscoelastic and across the direction of shear when the liquid is Newtonian (Petit and Noetinger [1988]). In a different kind of experiment involving steady flow without shear, Joseph, Nelson, Hu and Liu [1992] showed that large spheres with several millimeters in diameter sedimenting in a fluid-filled channel will arrange themselves so that the line of centers between neighboring spheres is across the stream in a viscous liquid and parallel to the stream in a viscoelastic liquid when the fall velocity is small but across the stream again when the fall velocity is large. They noted that this flow-induced anisotropy of sedimenting spheres is associated with the natural orientation of long bodies with their broadside parallel to the stream when viscoelasticity dominates and perpendicular to the stream when inertia dominates. Chains of spheres can also be seen in the sketches of the paper by Allen and Uhlherr [1989], but they were not identified in the text of that paper. In the present paper we focus on the orientation effects of sedimenting long bodies.

It is well known that the orientation of sedimenting long bodies in Stokes flow is undetermined; there are no hydrodynamic couples to turn a long body in steady flow. It is also known that flows of many different viscoelastic fluids reduce to Stokes flow when the flows are sufficiently slow and slowly varying. Turning couples appear at 2nd order.

Leal [1975] has studied the sedimentation of slender bodies in a second order fluid with inertia neglected. He considers only those non-Newtonian effects resulting from the disturbance velocity field generated by the lowest order geometry-independent approximation of the Stokeslet distribution used in slender body theory. He finds that freely translating particles with fore-aft symmetry exhibit a single stable orientation with the axis of revolution vertical. This suggests that the angle θ of tilt observed in experiments may be determined by a competition between inertia and viscoelasticity. The mechanism which aligns a slender body with the stream is not easy to extract from Leal's analysis.

Inertia cannot be neglected in a general discussion of the orientation of sedimenting long bodies. The streamwise orientation of a long body is unstable in a viscous liquid; the body will always turn its broadside to the stream. An explanation (Thompson and Tait [1879]) for this can be found in the couples which are produced by high pressures at the stagnation points on the long body shown in Figure 1. Potential flow is probably a good approximation for viscous flow on the forward side of the body. If the pressures outside a thin boundary layer at the stagnation points were reversed, the long body would not put its broadside into the stream, but instead would put its broadside parallel to the stream, as is in fact the case in the settling of long cylinders in various viscoelastic liquids. In practice, the wakes which develop on the back side of bodies give rise to a drag. The turning couples of such wake are self-equilibrating in symmetric cases ($\theta=0^\circ$ and $\theta=90^\circ$ in Figure 1) when the Reynolds number is small and the flow is steady, and self-limiting when the Reynolds number is large, due to vortex shedding (Hu, Joseph and Fortes [1992]).

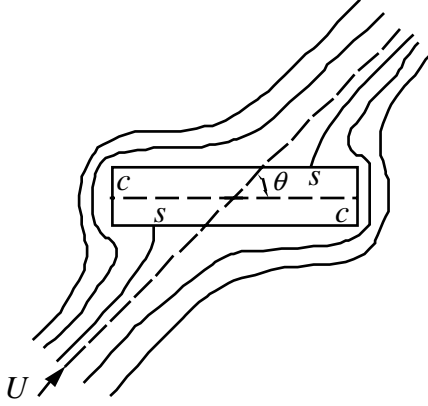


Figure 1. Potential flow past a cylinder. The pressure at stagnation points s will turn the broadside of the body into stream. If the extensional stress at s were reversed, as may be possible in a viscoelastic liquid, the body would line up with the stream. The same effect could be provided by normal stresses caused by strong shears at the corners c . In practice, viscosity will lead to boundary layers and wakes whose effects are not yet understood.

The orientation of a long body settling in a liquid under gravity is equivalent to the steady flow past a stationary long body. This latter problem has been treated in works of Ultman and Denn [1970], Joseph [1985], Crochet and Delvaux [1990], Hu and Joseph [1990] and Fraenkel [1988,1991]. These studies and related matters are discussed in the book of Joseph [1990]. The nonlinear studies were based on the upper-convected Maxwell model, but the linearized studies were basically model-independent. They show that the flow goes supercritical when the viscoelastic Mach number $M=U/c$ passes through one; the vorticity equation of the steady flow changes type from elliptic when $M<1$ to hyperbolic when $M>1$. In the supercritical case there is a Mach cone of vorticity. In front of the cone there is a "region of silence", actually potential flow, with vortical flow behind the cone. The supercritical transitions do seem to correspond to the flow transitions observed in the experiments on the flow over wires reported by James [1967], James and Acosta [1970] and Ambari, Deslouis and Tribollet [1984], as well as to the flow features observed in the experiments on flow over flat plates of Hermes and Fredrickson [1967].

It did not at first occur to us that the change of orientation of long bodies sedimenting in aqueous solutions of polyox could be framed as a change of type with features resembling those already seen in studies delayed die swell (see, Joseph [1990], henceforth called I). The cylinders settle vertically, more or less, when the Mach number is less than some number not too much greater than one. When the Mach number is larger than about three the particles have all turned their broadside to the stream, evidently controlled by inertia. Potential flow enters naturally into this description because there is an irrotational flow with a large upstream influence in front of the shock.

Joseph [1992] has shown that every potential flow is a solution of the equation of motion for second order fluid with stresses given by

$$\sigma_{ij} = -[C + \hat{\beta} \phi_{,il} \phi_{,il} - \rho \phi_{,t} - \rho |\mathbf{u}|^2/2] \delta_{ij} + 2[\eta + \alpha_1(\partial_t + \mathbf{u} \cdot \nabla)] \phi_{,ij} + 4(\alpha_1 + \alpha_2) \phi_{,il} \phi_{,lj} \quad (1.1)$$

where σ_{ij} is the active dynamic stress, C is a Bernoulli constant, $\hat{\beta} = 3\alpha_1 + 2\alpha_2$ is the climbing constant, ρ is the density, η is the viscosity, α_1 and α_2 are the quadratic constants, $\alpha_1 = -n_1/2$ and $\alpha_2 = n_1 + n_2$ with n_1 and n_2 being the first and second normal stress coefficients. In general, potential flow cannot satisfy no-slip conditions at solid walls. In this theory the streamlines are determined by the prescribed values of the normal component of velocity. You cannot see the effects that changing the values of the material parameters have on the values or distribution of the velocity in a potential flow. In the case of a rod rotating in a sea of second-order fluid, the potential-flow solution also satisfies the boundary conditions at the rod surface, and the potential flow is exact. Potential flows of viscous fluids exist outside boundary layer regions and separated regions behind bluff bodies. We have learned how to use potential flows in viscous flows and we must learn how to use them in viscoelastic flows.

The case of flow at the stagnation points of a body in steady flow is of special interest. The steady streaming past a stationary body is equivalent, under a Galilean transformation, to the steady motion of a body in an otherwise fluid. The quiescent streaming potential flow $(U, 0, 0)$ of a fluid near a point $(x_1, x_2, x_3) = (0, 0, 0)$ of stagnation is a purely extensional motion with principal rates of stretching

$$[\lambda_1, \lambda_2, \lambda_3] = \frac{U}{l} \dot{S} [2, -1, -1] \quad (1.2)$$

where \dot{S} is the half the dimensionless rate of stretching in the x_1 direction, l is the scale of length and

$$[u_1, u_2, u_3] = \frac{U}{l} \dot{S} [2x_1, -x_2, -x_3]. \quad (1.3)$$

In this case, $C = \frac{\rho}{2} U^2$, and we have

$$\begin{aligned} \begin{bmatrix} \sigma_{11} & 0 & 0 \\ 0 & \sigma_{22} & 0 \\ 0 & 0 & \sigma_{33} \end{bmatrix} &= \frac{\rho}{2} U^2 \left[\dot{S}^2 \frac{4x_1^2 + x_2^2 + x_3^2}{l^2} - 1 \right] \begin{bmatrix} 1 & 0 & 0 \\ 0 & 1 & 0 \\ 0 & 0 & 1 \end{bmatrix} + 2\eta \frac{U}{l} \dot{S} \begin{bmatrix} 2 & 0 & 0 \\ 0 & -1 & 0 \\ 0 & 0 & -1 \end{bmatrix} \\ &+ 2\frac{U^2}{l^2} \dot{S}^2 \begin{bmatrix} -\alpha_1 + 2\alpha_2 & 0 & 0 \\ 0 & -7\alpha_1 - 4\alpha_2 & 0 \\ 0 & 0 & -7\alpha_1 - 4\alpha_2 \end{bmatrix} \end{aligned} \quad (1.4)$$

At the stagnation point itself

$$\sigma_{11} = \frac{\rho}{2} U^2 + 4\eta \frac{U}{l} \dot{S} + 2(2\alpha_2 - \alpha_1) \frac{U^2}{l^2} \dot{S}^2. \quad (1.5)$$

Since $\alpha_1 < 0$ and $\alpha_2 > 0$, then $2\alpha_2 - \alpha_1 = \frac{5}{2} n_1 + 2n_2 > 0$ and the normal stress term in (1.5) is

positive independent of the sign of \dot{S} , but $4\eta\dot{S}$ is negative at the front side of a falling body and is positive at the rear. This is a new manifestation of the competition between inertia and normal stress, which may play a role in the flow-induced anisotropy. In practice we would not expect the symmetrical streamlines predicted by potential flow, but the normal stresses that are generated in the non-separated regions of flow around bodies may play an important role in the turning of long bodies and in the chaining of spherical bodies.

2. DIMENSIONLESS PARAMETERS

If we scale the stress with $\eta U/l$, then (1.4) may be written in terms of the dimensionless parameters

$$[\mathbb{R}, W_\alpha, A] = \left[\frac{Ul}{h/r}, \frac{U|\alpha_1|}{\eta l}, \frac{\alpha_2}{|\alpha_1|} \right] \quad (2.1)$$

where \mathbb{R} is a Reynolds number, W_α is a Weissenberg number defined in terms of a characteristic time $|\alpha_1|/\eta$, $\alpha_2/|\alpha_1|$ is the ratio of quadratic constants and

$$[\alpha_1, \alpha_2] = [-m, 2m-2] \hat{b}/(m-4) \quad (2.2)$$

where $m = 2\alpha_1/(2\alpha_1 + \alpha_2)$. It can be argued (I, chap.16) that $m=12.5$ is a reasonable value for our polyox solutions. Then $\frac{\alpha_2}{|\alpha_1|} = \left| \frac{2(1-m)}{m} \right| = \frac{23}{12.5}$ is a constant and α_1 and α_2 are determined by the measured values of the climbing constant \hat{b} .

The studies of supercritical flow around bodies discussed in the introduction could also be expressed in terms of \mathbb{R} and a Weissenberg number

$$W_\lambda = \frac{Ul}{\lambda} \quad (2.3)$$

which is defined for models like Maxwell's with single time of relaxation. For these models

$$\mathbb{R}W_\lambda = \frac{U^2}{(h/lr)} = \frac{U^2}{c^2} = M^2 \quad (2.4)$$

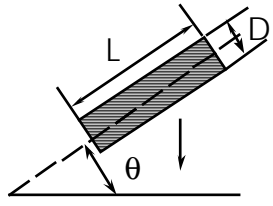
where $G = \eta/\lambda$ is the shear modulus, $c = \sqrt{G/r}$ is the shear wave speed and $M = U/c$ is the viscoelastic Mach number. We measure c directly on the wave speed meter (Joseph, Narain and Riccius. Part 1, Joseph, Riccius and Arney. Part 2 [1986], see I). The relaxation time $\lambda = \eta/\rho c^2$ taken from wave speed measurements is much smaller than the values obtained on conventional rheometers which typically filter out the high frequency response.

The parameters \mathbb{R} and W_λ are convenient for studies in which hyperbolicity and change of type are not relevant. When change of type is an important issue, it is better to use M and either

$$E = \frac{hl}{r l^2} \quad (\text{elasticity number}) \quad (2.5)$$

or W_λ as the fundamental parameters. The parameters are related, $W_\lambda = \mathbb{R}E$, $\mathbb{R} = M/\sqrt{E}$.

The choice of the scale of length l is ambiguous. We have adopted the convention that l is the hydraulic diameter (4 times the projected ($\theta=0^\circ$) area over the projected perimeter) calculated, for flat ended cylinders, by



$$l = \frac{4(DL\cos q + pD^2\sin q/4)}{2L\cos q + pD/2[1.5(1+\sin q) - \sqrt{\sin q}]} \quad (2.6)$$

for round ended ones, by

$$l = \frac{4[D(L-D)\cos q + pD^2/4]}{2(L-D)\cos q + pD} \quad (2.7)$$

and for cone ended ones, by

$$l = \frac{4[D(L-D)\cos q + pD^2\sin q/4]}{2(L-D)\cos q + pD/2[1.5(1+\sin q) - \sqrt{\sin q}]} \quad \text{when } q \geq 45^\circ \quad (2.8)$$

$$l = \frac{4[D(L-D)\cos q + pD^2\cos q/2]}{2(L-D)\cos q + 2D\sqrt{1+\cos^2 q}} \quad \text{when } q < 45^\circ \quad (2.9)$$

This choice of l ensures that the broadside-on configurations are all at Reynolds numbers greater than one. If $l > D$, then $l \varepsilon D$ with equality when $\theta = \pi/2$. We may say that inertial forces are greater than viscous forces when $\mathbb{R} > 1$.

Shape parameters which enter only weakly into the observations will not be considered.

3. MATERIAL PARAMETERS

The material parameters we need are the density ρ ($=1 \text{ g/cm}^3$), viscosity η (Figure 2), climbing constant \hat{b} and wave speed c . The climbing constant (Figure 3) is measured on a rotating rod viscometer (Beavers and Joseph [1975]). To compute \hat{b} from measured values of

the climb it is necessary to measure the surface tension. This was done with a spinning drop tensiometer (Joseph, et al [1992]) and the results are exhibited in Figure 4. The value of the tension is about 61 dyne/cm, close to that of distilled water, independent of the solution concentration from 0.5% to 1.5%. The value of \hat{b} is insensitive to small change of surface tension (I, chap.16).

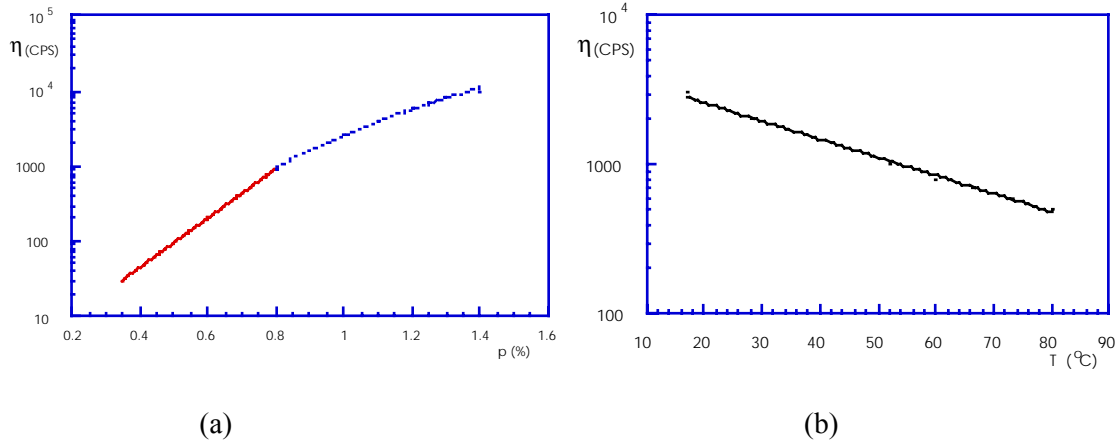


Figure 2. Measured zero shear rate viscosities η (cps) of aqueous solutions of polyox (Union Carbide, Products Manual [1981]). (a) solution viscosity at 25°C vs. percentage of polyox in water by weight. This curve was fitted to the formula $\eta = \{ \text{Error!} (2.1332 e^{7.5595p} \quad p < 0.8, 2546.1 p^{4.348} \quad p > 0.8 \text{ (dotted)})$ where p is percentage of polyox. (b) solution viscosity for 1% polyox vs. temperature T (°C), $\eta = 4532 e^{-0.028037T}$.

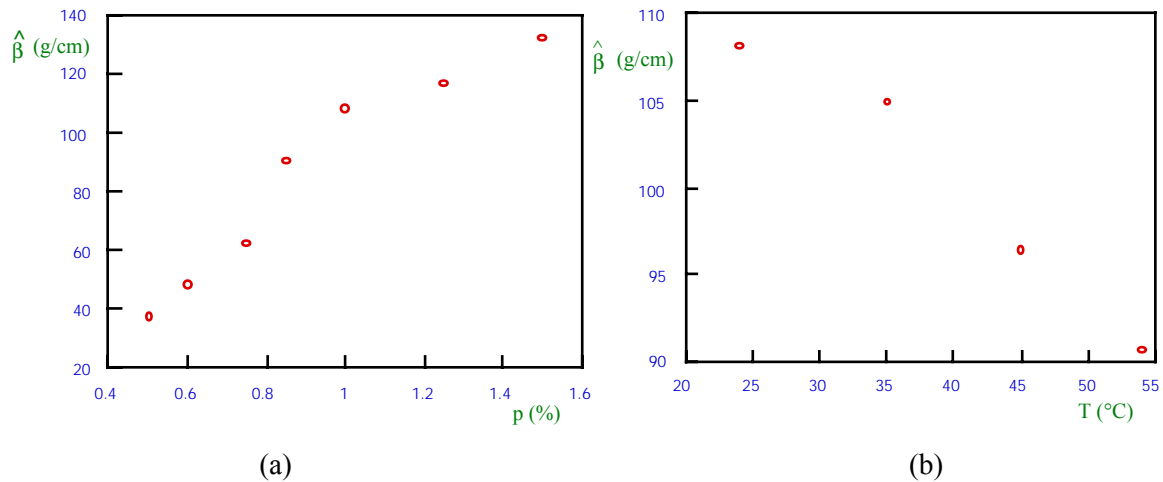


Figure 3. Climbing constants of aqueous solutions of polyox. (a) climbing constant vs. percentage of polyox in water at $T=24^\circ\text{C}$; (b). climbing constant of 1% polyox in water vs. temperature.

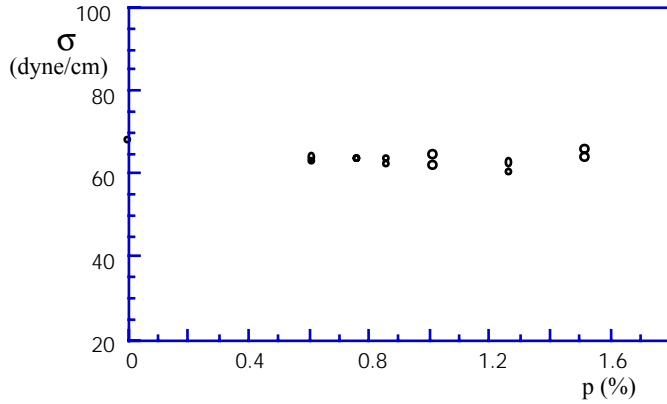


Figure 4. Surface tensions σ (dyne/cm) of aqueous solutions of polyox WSR-301 vs. percentage of polyox in water at room temperature.

Measured values of the wave speed are shown in Figure 5 and the physical properties of aqueous solutions of polyox WSR-301, whose molecular weight is approximately 4×10^6 , are listed in Table 1.

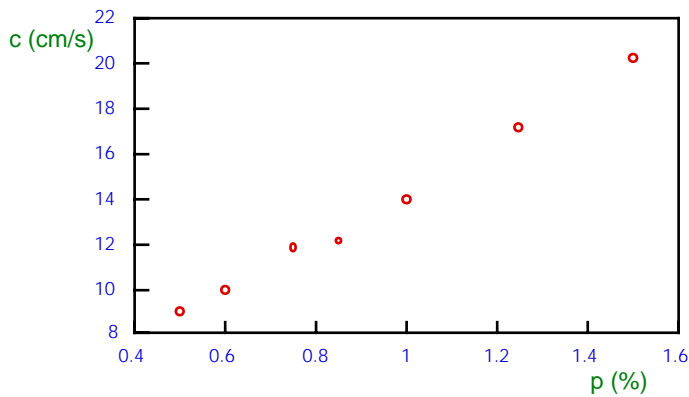


Figure 5. Shear wave speed c in aqueous solutions of polyox vs. percentage of polyox in water at room temperature.

The device used to measure the values in Figure 5 is a second generation wave speed meter which is basically a Couette device of the type described in appendix F of I. The new device has been simplified in various ways and it will be described in another publication. The values listed in Table 1 may be compared with the values listed on page 701 and 702 in I and the agreements are within the error bounds, approximately 30%. Certain theoretical issues with regard to wave speed have not yet been resolved. The speeds we measured correspond to the shear wave speed $c = \sqrt{G/r}$, one might expect to see in very soft rubbers, rather than to speeds of the order 10^5 cm/sec which

p(%)	T(°C)	η (ps)	σ (dyne/cm)	\hat{b} (g/cm)	α_1	α_2	c(cm/s)
------	-------	-------------	--------------------	------------------	------------	------------	---------

0.5	24	0.934		37.3	-54.83	100.93	9.05
0.6	24	1.99	61.5	48.5	-71.3	131.24	10.04
0.75	24	6.185	61.8	62.3	-91.58	168.58	11.88
0.85	24	12.56	60.9	90.6	-133.18	245.16	12.15
1	24	25.461	61.2	108.1	-158.91	292.52	14.04
	35	17.47		104.9	-154.2	283.86	
	45	12.834		96.4	-141.71	260.86	
	54	8.79		90.4	-133.33	245.43	
1.25	24	67.18	59.4	116.6	-171.4	315.52	17.24
1.5	24	148.43	63.3	132	-194.04	357.19	20.26

Table 1. Physical properties of polyox WSR-301/water solutions

are expected in the high frequency limits when the liquid responds as an elastic solid. The slow measured speeds presumably correspond to frequencies on a slowly varying portion of the storage modulus which may be approximated as a plateau. We don't believe there is a real plateau, so that different input frequencies should lead to different speeds. Moreover, the shear waves are dispersive so that we may see the spreading of any wave whose input is not a perfect step. In addition, the possible viscous effects of fast modes which have completely relaxed at the time scales of the experiments also need to be better understood. We are surprised more by the robustness of the measurements than by the scatter of the measurements. This may be due to the fact that the frequency of the impulse signal in our Couette meters may not excite greatly different speeds. And it is just the speeds which we measure on our meter which appear to correspond so well with dynamics in the problems of flow over bodies and delayed die swell reported in I as well as in the tilt angle transition reported here.

After obtaining the description of our data on the tilt angle transition in polyox solutions which leads to an interpretation in terms of a change of type, we decided to spot test this interpretation by dropping cylinders of the same length and shape but different weights and different diameters in a 2% solution of polyacrylamide in water. For this solution we obtained the values $\eta = 9$ ps, $c = 16.72$ cm/sec, $\sigma = 45$ dyne/cm, and $\hat{b} = 96.4$ g/cm at room temperature, where η is the zero shear rate viscosity. The polyacrylamide solution is very shear thinning as are the polyox solutions. The effective viscosity in our experiments could be as much a two or three times smaller than the zero shear rate value.

4. DESCRIPTION OF THE EXPERIMENTS

The properties of the cylinders used as test particles are listed in Table 2. The cone angle on the cylinders with cone ends is 90° . The difference between flat, round and cone ends can be understood at a glance from Figure 10 (in pages 23-24).

particle No.	diameter (in.)	length (in.)	material	cylinder shape	density (lb/in. ³)
1	0.25	0.4	plastic	flat ends	0.0476
2	--	0.6	--	--	--

3	--	0.8	--	--	--
3a	--	--	--	round ends	--
	0.1	--	--	--	--
	0.15	--	--	--	--
	0.35	--	--	--	--
	0.4	--	--	--	--
3b	0.25	--	--	cone ends	--
4	--	1	--	flat ends	--
5	--	0.4	teflon	--	0.0786
6	--	0.6	--	--	--
7	--	0.8	--	--	--
7a	--	--	--	round ends	--
7b	--	--	--	cone ends	--
8	--	1	--	flat ends	--
9	--	0.4	aluminum	--	0.0975
10	--	0.6	--	--	--
11	--	0.8	--	--	--
11a	--	--	--	round ends	--
	0.1	--	--	--	--
	0.15	--	--	--	--
	0.35	--	--	--	--
	0.4	--	--	--	--
11b	0.25	0.8	--	cone ends	--
12	--	1	--	flat ends	--
13	--	0.4	titanium	--	0.1621
14	--	0.6	--	--	--
15	--	0.8	--	--	--
15a	--	--	--	round ends	--
15b	--	--	--	cone ends	--
16	--	1	--	flat ends	--
17	--	0.4	tin	--	0.2633
18	--	0.6	--	--	--
19	--	0.8	--	--	--
19a	--	--	--	round ends	--
	0.1	--	--	--	--
	0.15	--	--	--	--
	0.4	--	--	--	--
19b	0.25	--	--	cone ends	--
20	--	1	--	flat ends	--
21	--	0.4	stainless steel	--	0.283
22	--	0.6	--	--	--

23	--	0.8	--	--	--
23a	--	--	--	round ends	--
23b	--	--	--	cone ends	--
24	--	1	--	flat ends	--
	0.017	0.8	--	--	--
25	0.25	0.4	brass	--	0.3063
26	--	0.6	--	--	--
27	--	0.8	--	--	--
27a	--	--	--	round ends	--
	0.1	--	--	--	--
	0.15	--	--	--	--
27b	0.25	--	--	cone ends	--
28	--	1	--	flat ends	--
29	0.3	0.4	--	--	--
30	--	0.6	--	--	--
31	--	0.8	--	--	--
31a	--	--	--	round ends	--
	0.35	--	--	--	--
	0.4	--	--	--	--
31b	0.3	--	--	cone ends	--
32	--	1	--	flat ends	--

note: "--" means same as above.

Table 2. Test particles

The cylinders were dropped in a liquid-filled channel, called a sedimentation channel, whose gap was slightly larger than the particle diameter. Two channels were used. The one used for the constant temperature experiments has a gap of 0.44 in., nearly twice the diameter of the smaller particle. This channel is 6.5 in. wide and 25 in. high. A second channel was used to test the effects of varying the temperature. This channel is 23 in. high, 4 in. wide with a gap of 0.275 in.. A heating mat was pasted to the one broad wall of the sedimentation channel facilitating uniform heating and the temperature of the mat could be controlled.

The motion of sedimenting particles in our three dimensional bed is basically two dimensional. The effects of closely spaced sidewalls in the experiments to be described are secondary. In our experiments the central axis of the cylinders always drifts to the plane midway between the closely spaced sidewalls, no matter what the initial condition. Even a thin wire needle with (D, L)=(0.017, 0.8) in. centers itself in this way.

Velocities and tilt angles were measured with a Kodak Spin Physics SP2000 Motion Analysis System which can take pictures at 2000 frames per second (fps). The image replayed is at a speed of 60 fps. Images can also be played in forward and backward at the rates of 2/3, 1, 3/2 or 3 fps, or one frame at a time. There are movable reticle lines which allow spatial measurements of the image. The elapsed time may be observed while a recording is being made and replayed. These functions allow one to measure the falling speed and tilt angle of sedimenting particle.

A schematic diagram of the experimental apparatus is shown in Figure 6.

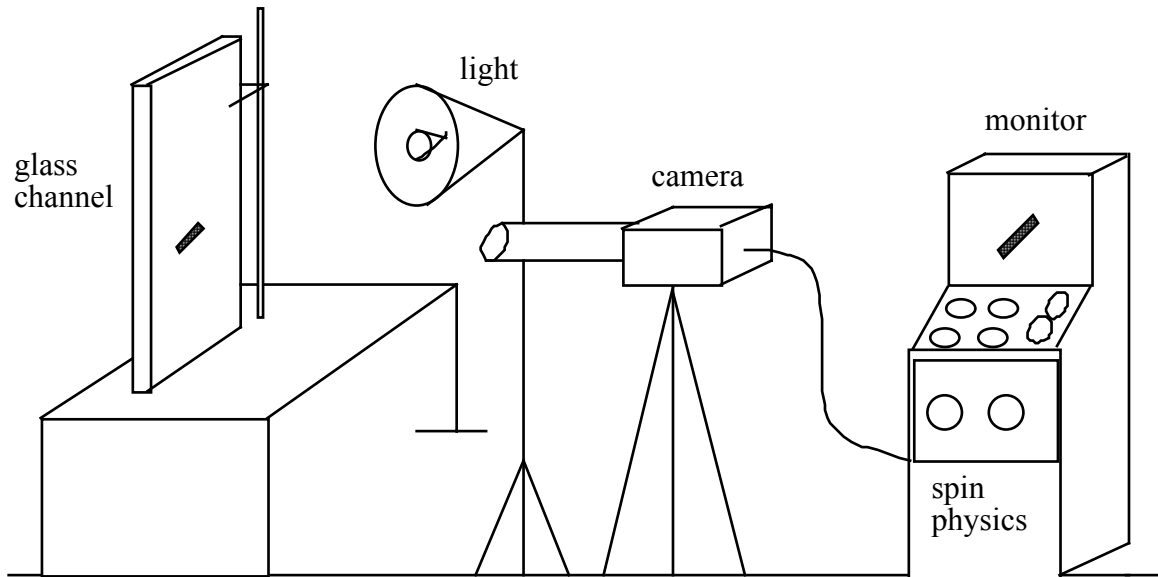


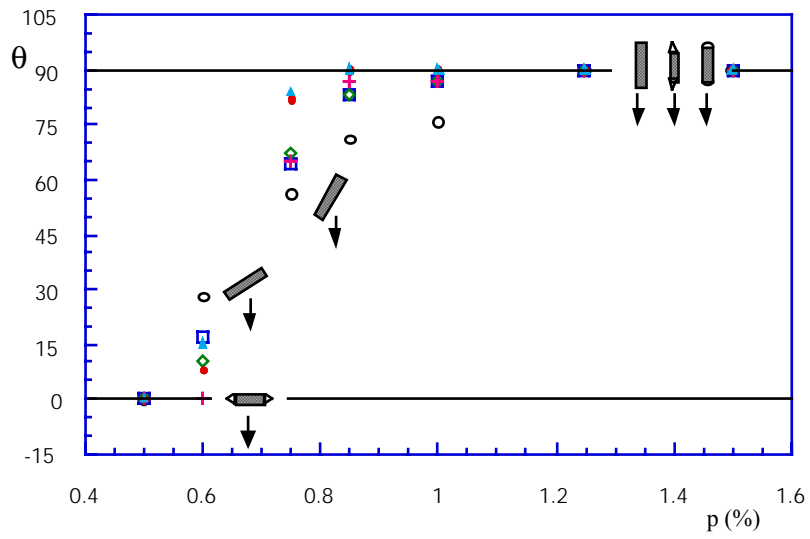
Figure 6. Schematic diagram of the experimental set-up.

5. TILT ANGLE TRANSITION

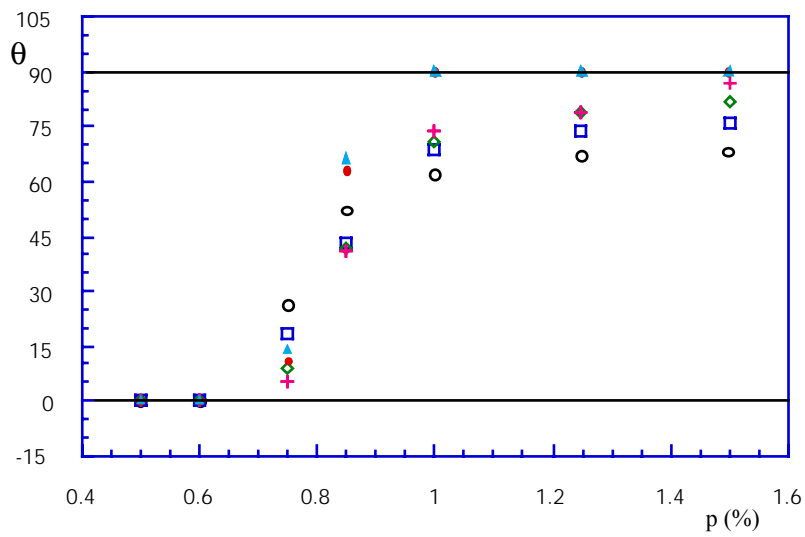
In this section we catalogue our observations of the tilt angle transition, from straight-down when normal stresses dominate to broadside-on when inertia dominates. We will look at the effects of changing the concentration, fall speed, particle length and diameter, particle shape and liquid temperature.

The 0.5% polyox/water solution is weakly viscoelastic. It climbs a rotating rod (see Table 1). In the sedimentation experiments the 0.5% solution behaves as if Newtonian: all particles sediment broadside-on. Since the viscosity of this solution is low, the fall speed is high. Viscoelastic effects are already strongly apparent in the 0.6% solution.

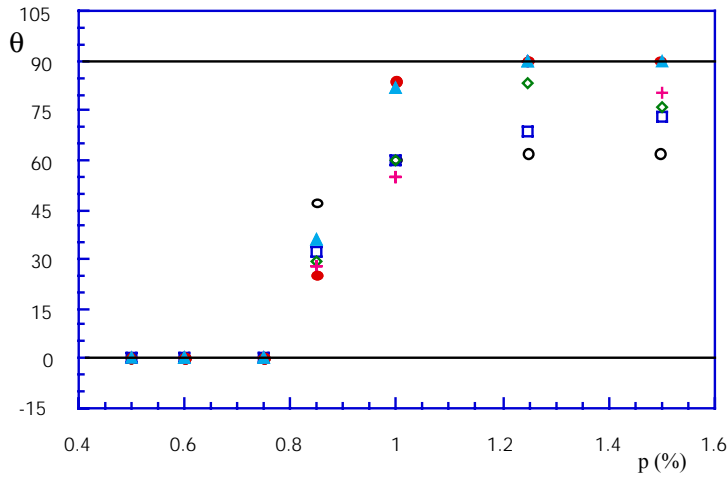
In Figure 7 we have plotted the variation of the tilt angle with concentration for four different cylinders ordered by weight. In all cases the tilt angle transition is a smooth function of concentration with broadside-on configurations ($\theta=0^\circ$) dominant at low concentrations where inertia dominates and straight-down configurations ($\theta=90^\circ$) dominant at high concentrations where normal stresses dominate.



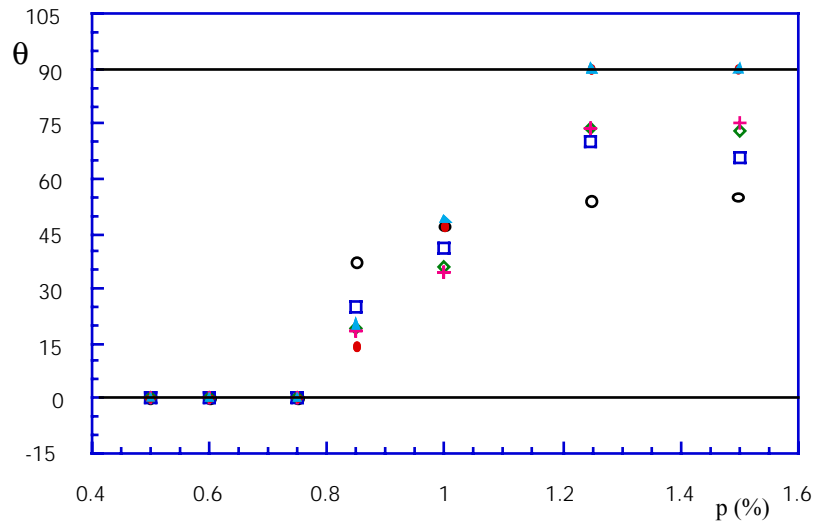
(a) teflon cylinders



(b) titanium cylinders



(c) tin cylinders



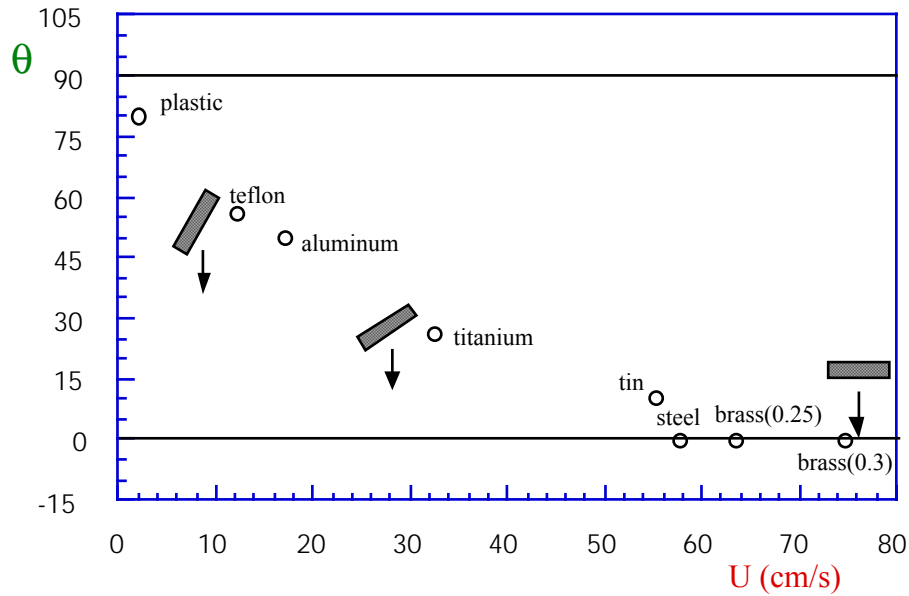
(d) brass cylinders (D=0.3 in.)

[-----]

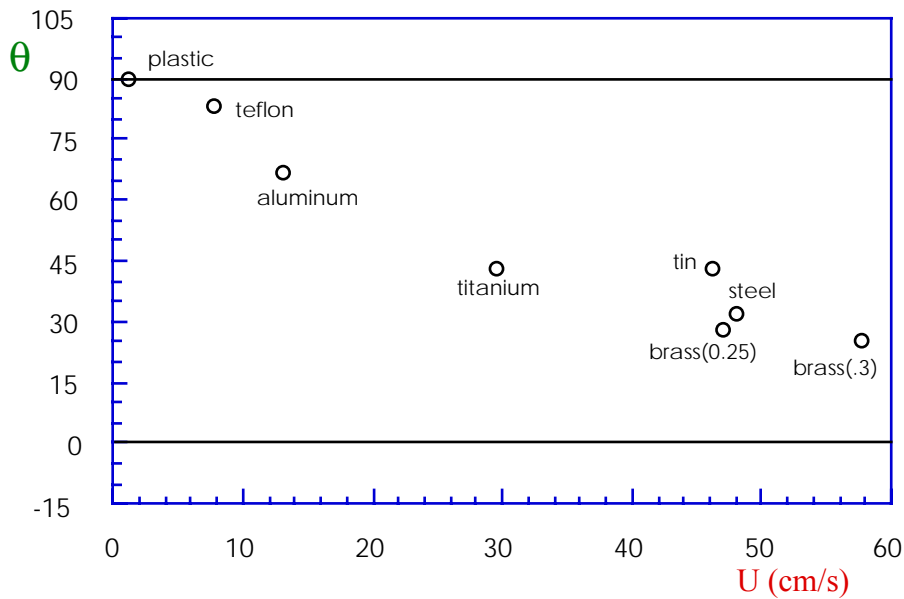
(1) 0.6% (2) 0.85% (3) 1.0% (4) 1.25% (5) 1.5%
 (e) titanium cylinders (D, L)=(0.25, 0.8) in. in different solutions

Figure 7 The effect of the concentration of polyox in water on the tilt angle ($T=24^{\circ}\text{C}$). (a) teflon, (b) titanium, (c) tin, (d) brass cylinders. When $\theta=0^{\circ}$ the motion is dominated by inertia; when $\theta=90^{\circ}$ the motion is dominated by normal stresses. As the concentration increases the tilt angle θ becomes larger. Figure 7(e) shows titanium cylinders with (D,L)=(0.25,0.8) in. falling in the aqueous solutions of polyox of various concentrations. \circ L=0.4 in., \square L=0.6 in., \diamond L=0.8 in., $+$ L=1 in. for flat ends, \bullet L=0.8 in. (round ends), \blacktriangle L=0.8 in. (cone ends).

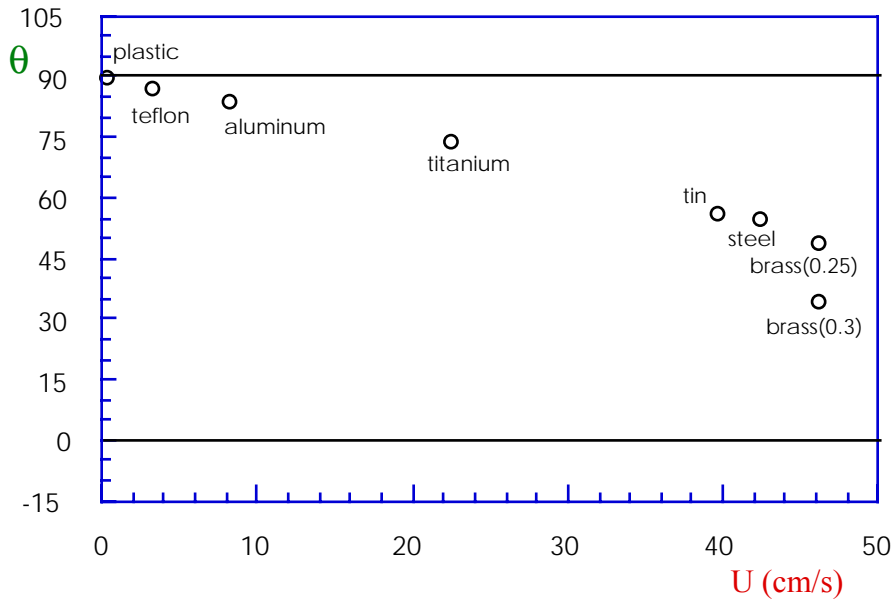
Inspection of Figure 7 indicates, as expected, that heavier cylinders are increasingly dominated by inertia, tending to settle broadside-on. This is even more strongly evident in Figure 8 in which the tilt angle is plotted as a function of fall velocity for different cylinders in solutions with different concentrations. Even the heavy cylinders fall slowly in concentrated, viscous solutions (see Figure 8(d)) and are dominated by normal stresses.



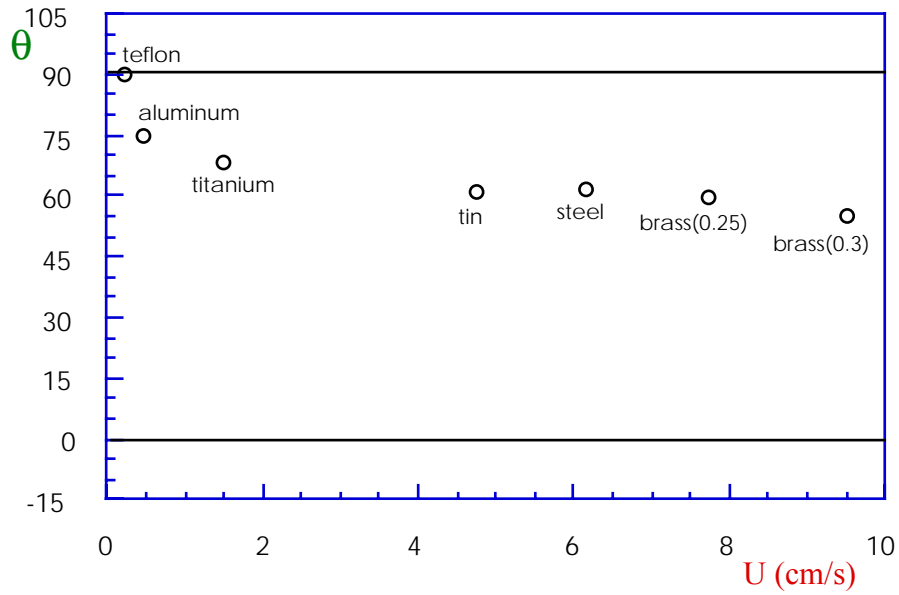
(a) cylinders with $L=0.4$ in. in 0.75% polyox



(b) cylinders with L=0.6 in. in 0.85% polyox



(c) cylinders with L=1.0 in. in 1.0% polyox



(d) cylinders with L=0.4 in. in 1.5% polyox

(1) plastic

(2) teflon

(3) aluminum

(4) titanium

(5) tin

(6) steel

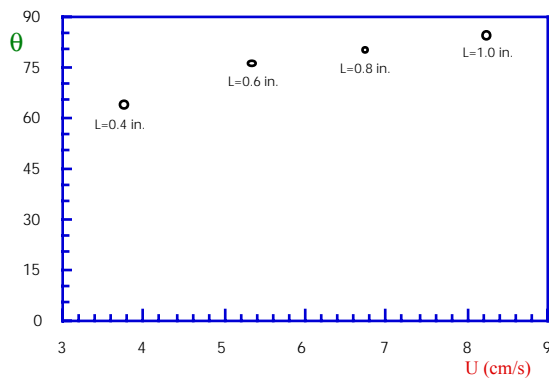
(7) brass(D=0.25 in.)

(8) brass(D=0.3 in.)

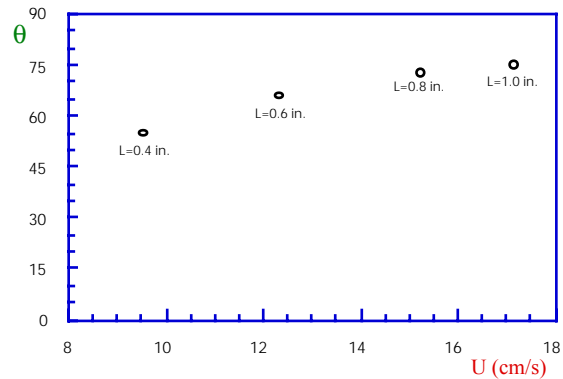
(e) cylinders with L=0.8 in. falling in 0.85% polyox

Figure 8 The effect of cylinder weight on the tilt angle ($T=24^{\circ}\text{C}$). (a) cylinders with same length $L=0.4$ in. but different densities falling in 0.75% polyox/water solution, (b) cylinders with $L=0.6$ in. in 0.85% polyox/water solution, (c) cylinders with $L=1.0$ in. in 1.0% polyox/water solution, (d) cylinders with $L=0.4$ in. in 1.5% polyox/water solution. The heavier the cylinder, the smaller the tilt angle. The pictures in Figure 8(e) show how cylinders with $L=0.8$ in. fall in 0.85% polyox/water solution.

We turn now to the effect of systematic changes in the length of the cylinders on the tilt angle. Four different lengths of 0.4 in., 0.6 in., 0.8 in. and 1.0 in. were tested. The typical results, shown in Figures 9(a), (b) and (c), are that longer cylinders fall at a larger tilt angle. But in lower concentration solutions normal stress effects are weak, so that when the fall speeds of particles are high their tilt angles are affected more by their weights than by their lengths. Then the longer cylinders may have smaller tilt angles, as shown in Figures 9(d), (e) and (f). One may also verify, from Figures 9(d) and (e), that when the normal stresses are relatively strong, as in the 1.0% polyox/water solution, and the fall speeds of cylinders are high, the tilt angles are determined by the joint effect of cylinder length and weight. When normal stresses are weak, solutions with concentrations lower than 0.75%, the tilt angle is affected more by cylinder weight than length. A longer cylinder may have a lower fall speed (Figure 9(e)) because it has a smaller tilt angle and experiences a greater drag.

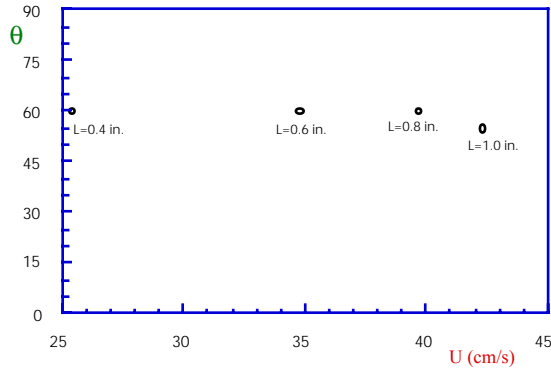


(a) aluminum cylinders in 1.0% polyox

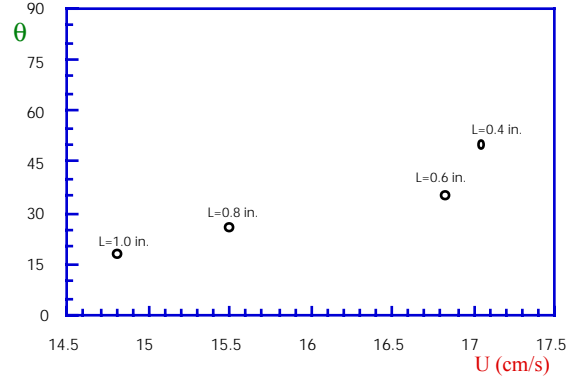


(b) brass cylinders (D=0.3 in.) in 1.5% polyox

- (1) L=0.4 in. (2) L=0.6 in. (3) L=0.8 in. (4) L=1.0 in.
(c) Titanium cylinders in 1.25% polyox



(d) steel cylinders
in 1.0% polyox

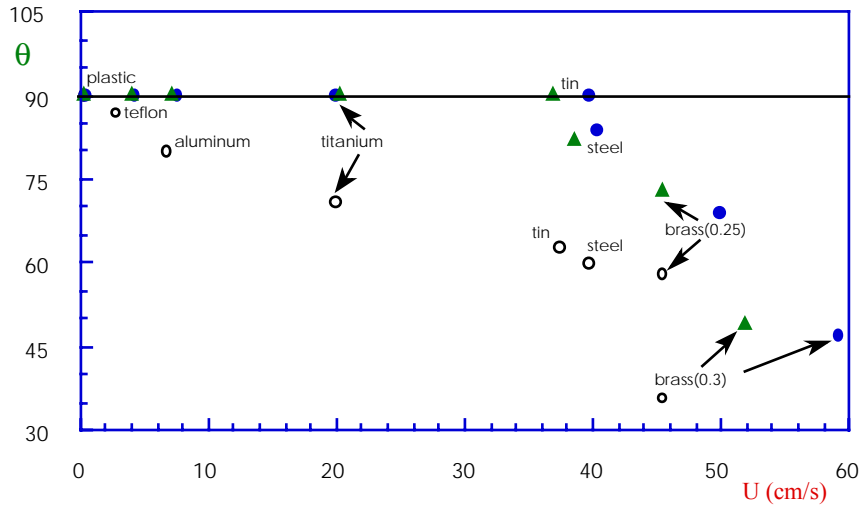


(e) aluminum cylinders
in 0.75% polyox

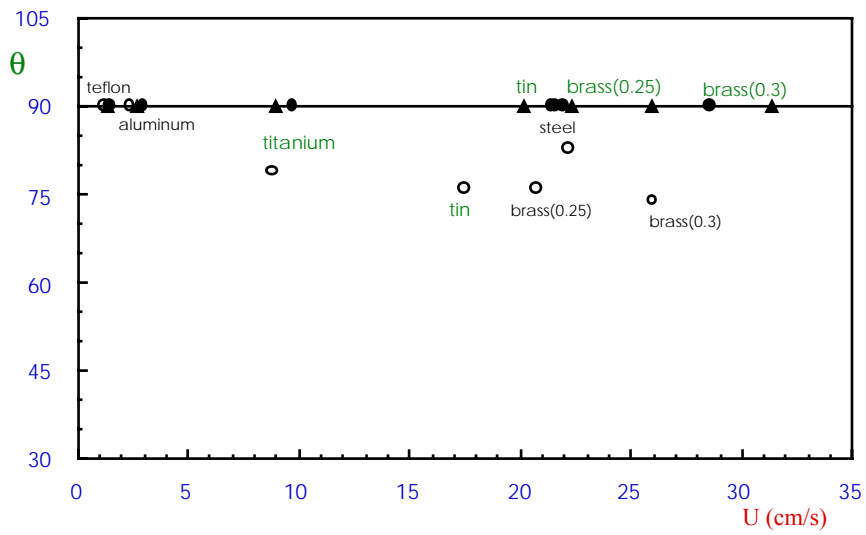
- (1) L=0.4 in. (2) L=0.6 in. (3) L=0.8 in. (4) L=1.0 in.
(f) teflon cylinders in 0.6% polyox

Figure 9. The effect of cylinder length on the tilt angle ($T=24^{\circ}\text{C}$). (a) aluminum cylinders in 1.0% polyox/water solution, (b) brass in 1.5% solution, (c) titanium in 1.25% solution, (d) stainless steel in 1.0% solution, (e) aluminum in 0.75% solution, (f) teflon in 0.6% solution.

The tilt angle of a cylinder is also affected by cylinder shape. The cylinders with round ends and cone ends always fall at larger tilt angles than the ones with flat ends (see Figure 10 and Figures 7(a)-(d)). The cylinders with flat ends have smaller tilt angles in general, other things being equal. It is possible that forces are generated at sharp corners which may generate tilt angles from small imperfections even when inertial effects are small.



(a) cylinders with $L=0.8$ in. in 1.0% polyox



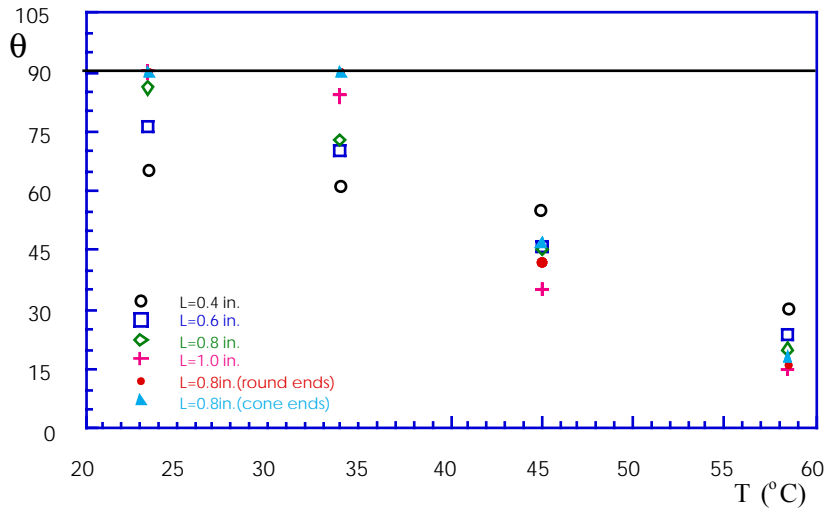
(b) cylinders with $L=0.8$ in. in 1.25% polyox

(1) flat ends (2) round ends (3) cone ends
(c) brass cylinders with (D, L)=(0.25, 0.8) in. in 1.0% polyox

(1) flat ends (2) round ends (3) cone ends
(d) brass cylinders with (D, L)=(0.25, 0.8) in. in 1.5% polyox

Figure 10. The effect of cylinder shape on the tilt angle ($T=24^{\circ}\text{C}$). (a) cylinders with same length $L=0.8$ in. but with flat ends, round ends and cone ends respectively, falling in 1.0% polyox/water solution, (b) the same cylinders falling in 1.25% solution, (c) and (d) brass cylinders falling in 1.0% and 1.5% solutions. \circ flat ends, \bullet round ends, \blacktriangle cone ends.

Figure 11 shows the effect of temperature on the tilt angle. The effect of increasing the temperature is equivalent to the effect of decreasing the concentration of the solution, as is evident already from inspection of Table 1.



(a) tin cylinders in 1.0% polyox

- (1) T=23.5°C (2) T=34°C (3) T=45°C (4) T=58.5°C
 (b) brass cylinder with (D, L)=(0.25, 1.0) in. in 1.0% polyox

Figure 11. The effect of liquid temperature on the tilt angle. (a) tin cylinders falling in 1.0% polyox/water solution at different temperatures, (b) a brass cylinder with (D, L)=(0.25, 1.0) in. in 1.0% polyox/water solution at different temperatures. As the temperature increases, the tilt angle decreases.

In §6 we shall organize the data on the tilt angle transitions in the frame of the dimensionless variables defined in §2. We shall see that this transition from straight-down orientations when the viscoelastic Mach number is less than one to broadside-on orientations when the Mach numbers are greater than a number between one and four may be explained as a change of type.

The idea that the tilt angle transition is the consequence of a change of type, in which the vorticity equation is elliptic when inertia is small and hyperbolic when inertia is large, requires further study. It would be best if the results of the present study could be checked in another laboratory. The experiments are relatively simple and the observable tilt angle and fall speeds are unambiguous. The down side for independent verification is that the data correlates well with the measurements of the wave speed from the wave speed meter (US patent 4,602,502) which at present exists only in our laboratory.

After obtaining the description of our experimental results on the tilt angle transition in aqueous polyox solutions which leads to an interpretation in terms of change of type, we decided to spot test the interpretation by redoing experiments with very small diameter cylinder, (D, L)=(0.017, 0.8) in., and by dropping cylinders of same length and shape (most cylinders with round ends, only a few with flat ends) but different diameters and weights in a 2% solution of polyacrylamide and water. When the thin cylinder is dropped in 1.5% aqueous polyox with its axis perpendicular to gravity it will sediment very slowly and gradually turn to the straight-down position. In this case $M \ll 1$ and $\mathbb{R} \ll 1$. When it falls in 0.5% aqueous polyox, it will turn its broadside to the stream. Here $(M, \mathbb{R}) \sim (2, 1.6)$ consistent with a change of type. We also dropped some rectangular plates in a three-dimensional channel filled with 2% aqueous polyacrylamide. The lighter ones fall straight-down, the heavier ones fall broadside-on and the ones between will fall with a tilt angle.

The tilt angle response in the experiments on sedimentation of cylinders with length of L=0.8 in. in the 2% aqueous polyacrylamide solution is described in Table 3.

material	D(in.)	\square	U(cm/s)	\mathbb{R}	M	E	E_{\square}	W_{\square}	W_{\square}
plastic	0.1	90	0.47	0.01	0.03	4.536	2218.1	0.060	29.28
--	0.15	90	0.78	0.03	0.05	1.987	971.54	0.066	32.16
--	0.25	90	1.34	0.09	0.08	0.716	350.30	0.068	33.17
--	0.25	90	1.09	0.08	0.07	0.719	351.50	0.055	27.03
--(f)	0.25	90	1.08	0.08	0.06	0.722	353.30	0.055	26.85
--	0.35	90	0.98	0.10	0.06	0.367	179.69	0.036	17.38

--	0.4	90	0.99	0.11	0.06	0.285	139.17	0.032	15.45
teflon	0.25	90	8.49	0.60	0.51	0.719	351.47	0.431	210.53
--	0.25	90	7.54	0.53	0.45	0.719	351.44	0.382	186.96
--(f)	0.25	90	7.19	0.71	0.43	0.372	181.97	0.262	128.29
aluminum	0.1	90	4.01	0.11	0.24	4.506	2203.2	0.509	248.96
--	0.15	90	8.02	0.34	0.48	1.991	973.46	0.677	330.98
--	0.25	90	14.94	1.05	0.89	0.724	354.20	0.761	371.91
--	0.25	90	14.37	1.01	0.86	0.724	354.16	0.731	357.70
--(f)	0.25	90	13.09	0.92	0.78	0.718	351.13	0.663	324.44
--	0.35	53	18.27	3.58	1.09	0.093	45.57	0.334	163.13
--	0.4	31	16.82	3.97	1.01	0.064	31.40	0.255	124.68
titanium	0.25	8	20.00	5.32	1.20	0.051	24.73	0.269	131.55
--	0.25	4	18.68	2.71	1.12	0.170	83.13	0.461	225.27
--	0.25	0	20.00	2.23	1.20	0.288	140.73	0.642	313.82
--(f)	0.25	13	19.98	1.88	1.19	0.403	196.98	0.758	370.91
--(f)	0.25	11	18.54	1.76	1.11	0.396	193.70	0.698	341.30
tin	0.1	85	27.31	0.25	1.63	41.36	20225.7	10.51	5137.3
--	0.1	88	27.19	0.19	1.63	76.45	37387.0	14.22	6954.0
--	0.15	4	19.69	1.44	1.18	0.669	327.11	0.963	471.04
--	0.25	0	41.64	4.65	2.49	0.287	140.30	1.334	652.37
--	0.25	0	39.69	4.43	2.37	0.287	140.44	1.272	622.14
--(f)	0.25	0	37.35	4.02	2.23	0.309	151.33	1.243	607.74
--	0.4	0	60.48	9.48	3.62	0.146	71.21	1.380	675.06
steel	0.25	0	45.36	5.07	2.71	0.286	140.04	1.452	710.01
--	0.25	0	40.10	4.48	2.40	0.287	140.17	1.284	627.97
--(f)	0.25	0	43.05	4.31	2.57	0.357	174.55	1.538	752.31
brass	0.1	90	33.87	0.96	2.03	4.491	2196.1	4.293	2099.4
--	0.15	0	24.66	1.81	1.47	0.664	324.76	1.202	587.81
--	0.25	0	48.85	5.46	2.92	0.286	140.05	1.564	764.65
--	0.25	0	47.37	5.29	2.83	0.287	140.29	1.518	742.13
--(f)	0.25	0	44.56	4.79	2.67	0.309	151.34	1.483	725.09
--	0.3	0	60.48	7.76	3.62	0.217	106.27	1.686	824.69
--	0.3	0	57.73	7.40	3.45	0.218	106.48	1.611	787.95

--(f)	0.3	0	54.04	6.66	3.23	0.236	115.33	1.570	767.62
--	0.35	0	68.65	9.83	4.11	0.174	85.33	1.715	838.79
--	0.4	0	72.57	11.4	4.34	0.145	70.90	1.653	808.23

note: "--" means same as above, (f) indicates the cylinders with flat ends, E_α is elasticity number defined in terms of a relaxation time $\lambda=|\alpha_1|/\eta$.

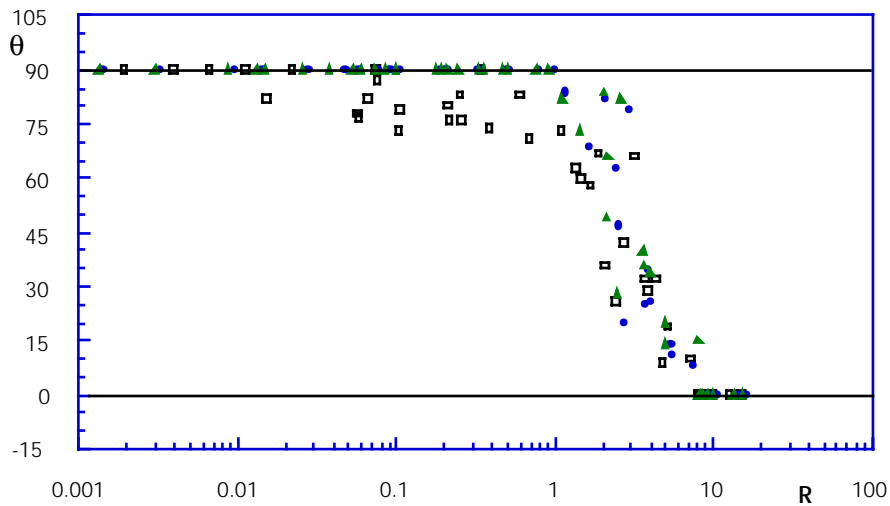
Table 3. Tilt angle response of sedimenting cylinders in 2% aqueous polyacrylamide (Cyanamer N-300 LMW) at room temperature. The zero shear viscosity is $\eta = 9$ poise. The molecular weight is about 5×10^6 . The value of the shear-wave speed measured on the wave speed meter is $c=16.72$ cm/sec. The surface tension and climbing constant are $\sigma=45$ dyne/cm and $\hat{\beta} = 96.4$ g/cm respectively.

6. CORRELATIONS OF THE TILT ANGLE TRANSITION

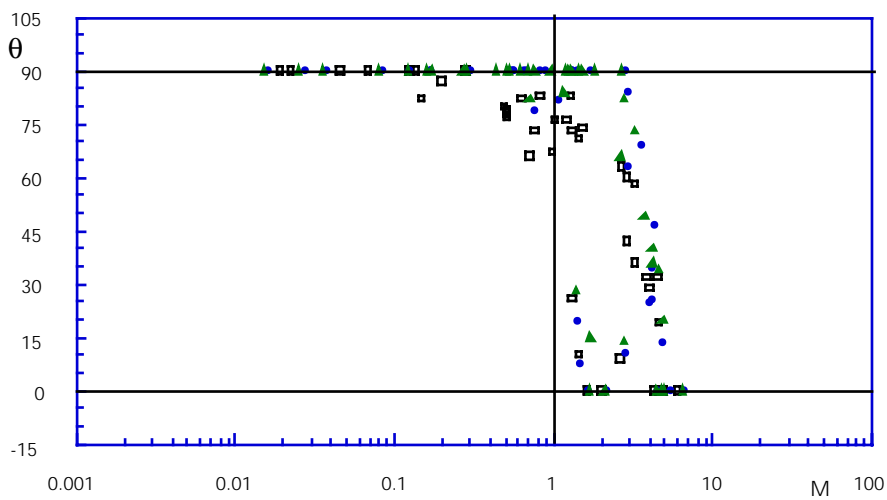
In this section we shall show how the tilt angle transition correlates with Reynolds number and Mach number. The definition of the Reynolds number is ambiguous because there is no natural choice for the length scale and because the effective viscosity in each realization depends on an effective rate of shear, which we have not determined. It is probable that the zero shear rate viscosity is perhaps three times larger than the effective viscosities of sheared fluids in the experiments. In Figures 12(a), 13(a) and 14(a) we used the zero shear viscosity so that the effective Reynolds numbers are two or three times larger than these shown.

Figures 12, 13 and 14 show that the tilt angle transition requires at least that the Reynolds number should be sufficiently large and the Mach number larger than one. For Newtonian liquids $\mathbb{R} > 0.1$ is sufficiently large for complete turning in our experiments. In general, it is probable, and our two-dimensional simulations show that no matter how small $\mathbb{R} > 0$ may be the cylinders will eventually turn broadside-on.

The Mach number correlation (Figures 12(b), 13(b) and 14(b)) is perhaps more interesting because it is motivated by theory and because the Mach number is based only on directly measured quantities: the terminal velocity and



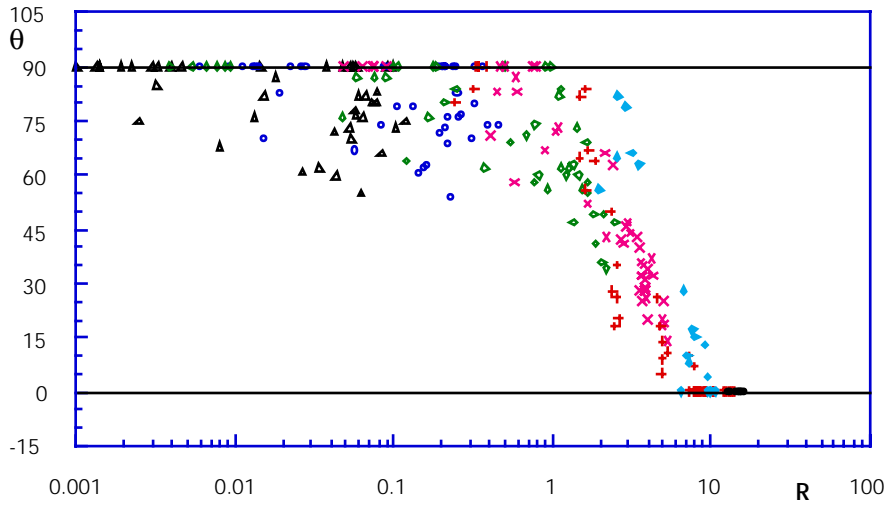
(a)



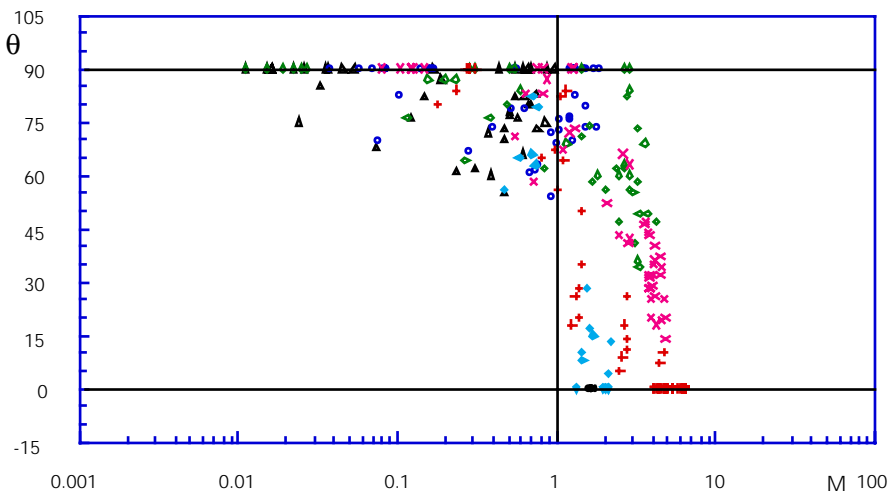
(b)

Figure 12. Tilt angle θ vs. Reynolds number (a) and tilt angle vs. Mach number (b) for cylinders with $L=0.8$ in. in polyox/water solutions of various concentrations. \square flat ends, \bullet round ends, \blacktriangle cone ends.

the wave speed measured on our wave speed meter. The Mach number criterion is very demanding since it requires that a transition depends on the size, shape and weight of particles and on the other parameters determining drag only through the value of the terminal velocity. The physics behind this is



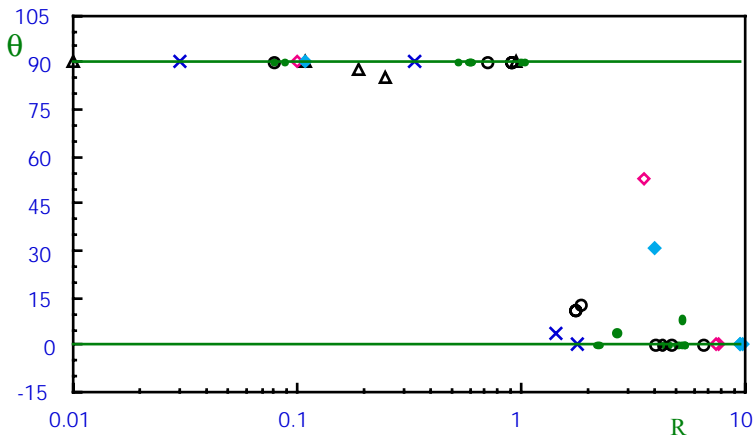
(a)



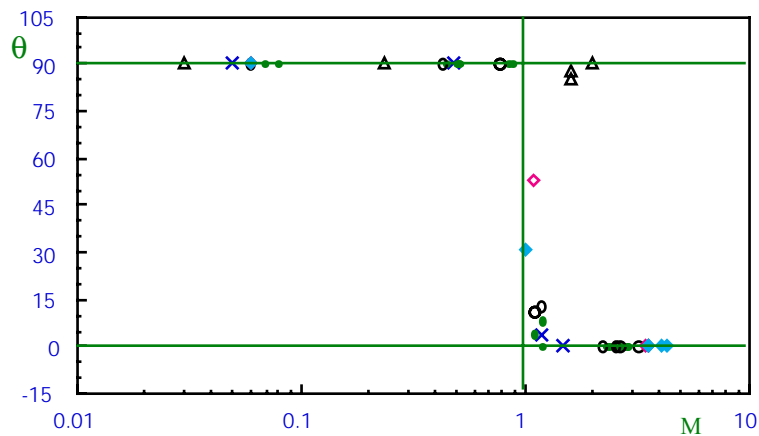
(b)

Figure 13. Tilt angle θ vs. Reynolds number (a) and tilt angle vs. Mach number (b) for all the data, cylinders of all lengths, shapes and weights in polyox/water solutions: Δ 1.5%, \circ 1.25%, \diamond 1%, \times 0.85%, $+$ 0.75%, \blacklozenge 0.6%, \bullet 0.5%.

that when $M > 1$, waves of velocity (shear waves) cannot propagate upstream. The vorticity is confined to a region behind a shock which terminates in a Mach cone and the flow in front of the shock is irrotational. It is possible that the potential flow at the front of the body in the supercritical case is a source for the turning couples which produce the tilt-angle transition to the broadside-on configuration.



(a)



(b)

Figure 14. Tilt angle θ vs. Reynolds number (a) and tilt angle vs. Mach number (b) for cylinders with $L=0.8$ in. (most with round ends) in 2% aqueous polyacrylamide, Δ $D=0.1$ in., \times $D=0.15$ in., \bullet $D=0.25$ in., \circ $D=0.25$ in. (flat ends), \diamond $D=0.35$ in., \blacklozenge $D=0.4$ in.

It is not possible for the dynamics of a viscoelastic fluid to be determined only by the Mach number. The simplest model (say the telegraph equation (5) on p.212 in I) depends on a Mach number M and changes type when M passes through one, but the damping term depends on the Weissenberg number $W\lambda$; it is small when the memory is long, i.e., when $W\lambda$ is large. Having said this, we are compelled to call attention to the abrupt and clean dependence of the tilt angle transition on the Mach number in the polyacrylamide solution (Figure 14(b)). In the flow of an upper convected Maxwell fluid over a cylinder there is a "bow" shock in front of the cylinder (see Figures 7.1 and 7.12 in I) and the flow can be locally supercritical in regions away from the body even when the Mach number based on the free stream is subcritical. This may explain the appearance of tilt angle less than 90° when $M < 1$. The appearance of such tilt angles

is particularly apparent for the sharp end cylinders and the most concentrated solution where the turning couples due to large normal stresses may be important even when $M < 1$. The structure of a supercritical flow over a tilted cylinder is certainly a complicated and interesting problem which should be amenable to numerical analysis.

We have noted already that the preceding considerations do not apply to Newtonian liquids or then, obviously to weakly non-Newtonian liquids. We are uncertain about the criteria we ought to apply to distinguish non-Newtonian from Newtonian liquids. Joseph [1990] argued that the effective Newtonian viscosity μ in a Jeffreys' model

$$\lambda \overset{\Delta}{\boldsymbol{\tau}} + \boldsymbol{\tau} = 2\eta \mathbf{D}[\mathbf{u}] + 2\mu \lambda \overset{\Delta}{\mathbf{D}} \quad (6.1)$$

is relatively small in liquids that are effectively viscoelastic, with well defined wave speeds $c = \sqrt{h/\lambda r}$. The effective Newtonian viscosity arises from the decay of fast modes.

If $\mu=0$, then (6.1) is a Maxwell model, and if μ/η is small, then (6.1) is a perturbed Maxwell model, with Δ representing an "invariant" derivative, say a covariant derivative. The normal stresses are embedded in the nonlinear terms defining this derivative, so that if λ is large, the normal stresses are large.

If the ratio μ/η of the Newtonian to the elastic viscosity is close to one the liquid is a perturbed Newtonian fluid with a small elastic viscosity. These fluids will respond like Newtonian liquids with inertia effects controlling orientation even when the ratio \mathbb{R} of inertia to viscous forces is surpassingly small.

The existence of a window of Mach numbers near one in which the tilt angle transition takes place reminds us of delayed die swell (Joseph, Matta and Chen [1987], see Chap.13 in I). In that problem the delay was initiated only at supercritical Mach numbers and the swell was gradual. In the fully swelled region the Mach number was always subcritical $M < 1$. It follows that there is always a point in the region in which the swelling is not complete where $M = 1$. The Mach number in this region is changing locally from $M > 1$ to $M < 1$. This swelled region then frames a window of Mach numbers. In the problem of delayed die swell hyperbolic transitions were observed in all of 19 very different polymer liquids tested. In these experiments it was argued that the smoothing of the delayed swell in some of the liquids could be attributed to the action of an effective Newtonian viscosity. It is certain that many people have seen delayed die swell, but they cannot check the details of the transition without measuring shear wave speed c . Gas dynamics would perhaps look good on paper, but only there, if we could not measure the speed of sound. We are betting that the tilt angle transition is universally a change of type and think it best to wait for others to prove us wrong.

7. ANOMALOUS ROLLING OF A SPHERE IN A VISCOELASTIC FLUID DOWN AN INCLINED WALL

In this experiment, we tilted our sedimentation channel with its center plane vertical and the side walls inclined to vertical. The channel is filled with liquid. A sphere is placed on the inclined wall and it falls under its own weight while rolling. In Newtonian fluids the sense of the

rotation is the same as if the sphere were rolling down an inclined plane in air. But in non-Newtonian fluids the sphere can rotate in the other direction while it falls (Joseph, Nelson, Hu and Liu [1992]). In this section we shall give a precise quantitative description of this phenomenon for aqueous polyox solutions, but the phenomenon is generic and occurs in many polymer liquids.

In the polyox solutions we were able to obtain reproducible data exhibiting anomalous rolling only in the more concentrated solutions: 1.5%, 1.25% and 1%. Anomalous rolling occurs in the 0.85% solution, 0.75% is ambiguous and only normal rolling occurs in the more dilute solutions and in all Newtonian liquids. In the more concentrated solutions we were able to change the fall velocity and the angular velocity of the rolling sphere by putting a wire on the inclined wall so that the sphere would roll on the wire. The angular speed is relatively large in the 1.5% solution when there is a wire on the inclined plane, but this tendency is not so marked in the 1.25% solution (see Figure 15(a)). When the inclination of the wall with respect to the horizontal is smaller than a certain value which depends on the solution concentration, a falling sphere reverses its direction of rotation. If a sphere is dropped a small distance from a vertical wall in a viscoelastic liquid, it will move to the wall and rotate in the counterintuitive sense as it falls. But the same sphere dropped in a viscous liquid will move away from the vertical wall.

Figure 15 summarizes the data for anomalous rolling. Figure 15(a) is a plot of the angular speed against the angle of inclination of the wall from the horizontal. The closer the inclination is to vertical, the faster is the rotation in the counterintuitive sense. In Figure 15(b) we have plotted the angular speed Ω against the Reynolds number $\mathbb{R}=UD\rho/\eta$, where U is the falling velocity along the inclined wall, D is the diameter of the sphere and, η is the zero shear rate viscosity. The anomaly is that the faster it falls, the faster it rotates in the wrong sense. We have basically three straight lines with same slope in a semi-log plot. We can fit the data to the form

$$\Omega = a + 1.08\text{Log}(\mathbb{R}) \quad (7.1)$$

with an a which does not vary strongly with concentration between 1% and 1.5% and is given by

$$a = 0.3718 + 1.311\text{Log}(E) \quad (7.2)$$

where

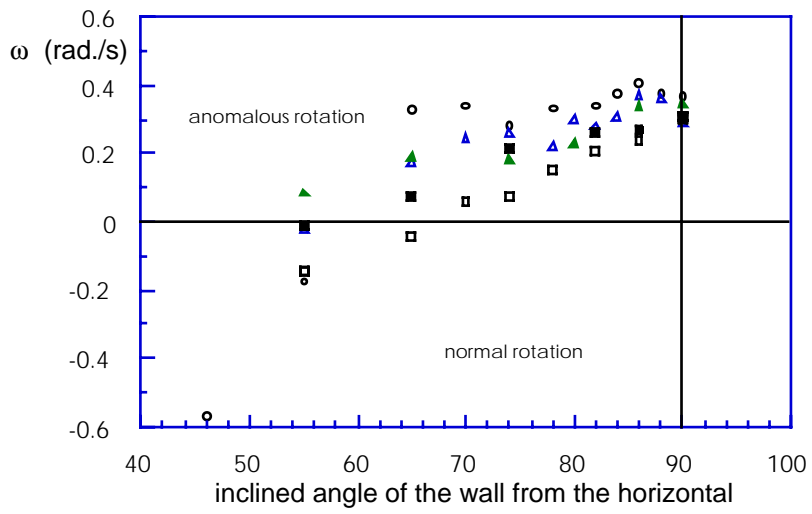
$$E = \frac{hl}{rD^2} \quad (7.3)$$

and

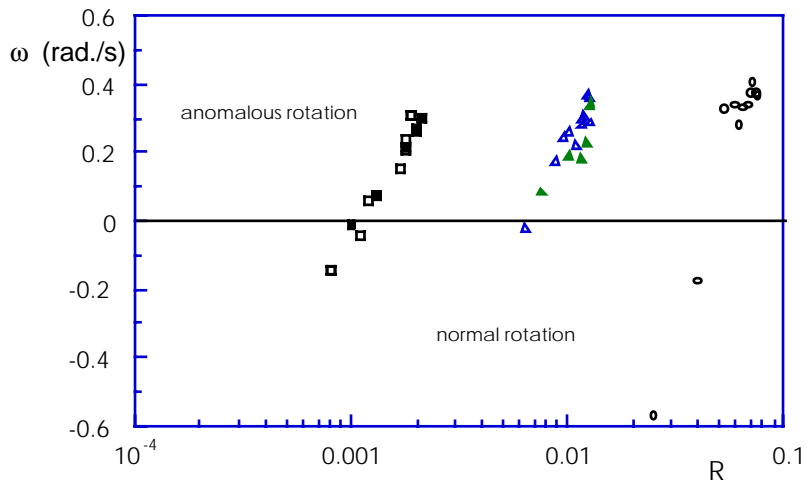
$$\lambda = \frac{h}{rc^2} \quad (7.4)$$

is a relaxation time. When we put these fits together, the data collapses around the line

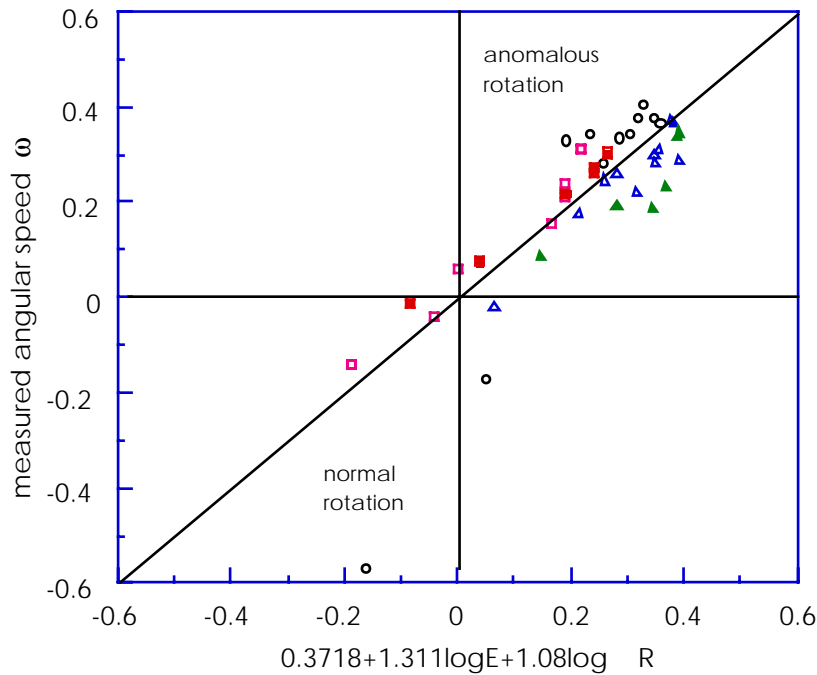
$$\Omega = 0.3718 + 1.311\text{Log}(E) + 1.08\text{Log}(\mathbb{R}) \quad (7.5)$$



(a)



(b)



(c)

Figure 15. Anomalous rolling of a sphere on a wall inclined from the vertical in polyox/water solutions: (a) angular speed ω vs. the angle of inclination from horizontal (90° is vertical). (b) ω vs. \mathbb{R} . (c) measured ω vs. calculated ones from the correlation (7.5). \circ 1% polyox, flat surface; \triangle 1.25% polyox, flat surface; \blacktriangle 1.25% polyox, wire surface; \square 1.5% polyox, flat surface; \blacksquare 1.5% polyox, wire surface.

The correlation (7.5) and our observations suggest that anomalous rolling is a slow flow phenomenon, perhaps well described as a perturbation of Stokes flow.

The reader should not interpret the graphs in Figure 15 to mean that anomalous rolling is more pronounced in dilute solutions. The angular speed of rolling and the fall velocity of spheres are greater in the 1% solution because the viscosity is smaller. Spheres never rotate in any but a normal manner in dilute solutions and Newtonian liquids.

8. CONCLUSIONS

(1). It is well known that a long body settling in a viscous liquid will turn its broadside to the stream. The same long body settling in a viscoelastic fluid will turn its broadside parallel to the stream but heavier long bodies which fall faster again turn broadside.

- (2). There is a regime in which viscoelastic stresses and inertia compete. This competition evidently decides the tilt angle which the axis of a long body makes with the direction of fall in steady flow. No matter how the body is oriented initially, it will eventually fall with a unique angle of tilt.
- (3). The tilt angle can be controlled by changing the concentration of the solution using the same long particle or by changing the weight of the particle in the same solution. In concentrated solutions the long body settles straight-down. In dilute solutions it settles broadside-on.
- (4). The shape of the ends of the cylinder has an effect on the tilt angle, with rounded ends giving a larger angle of tilt (from the horizontal), as in the viscoelastic case. Sharp ends give rise to more erratic behavior than smooth ones, with small tilt angles arising in situations where cylinders with smooth ends settle straight-down. This erratic behavior may be due to large normal stresses at the sharp corners.
- (5). In concentrated solutions, long cylinders have a larger tilt angle and settle straight-down. The tilt angle of long cylinders falling in more dilute solutions is more affected by the higher terminal velocity which induces inertial effects and a smaller tilt angle.
- (6). Increasing the temperature of a solution has the same effect on the tilt angle as decreasing the concentration.
- (7). Particles center themselves rigorously between the two close walls of sedimentation channel. The center appears to be a global attractor.
- (8). The tilt angle transition appears to be a critical transition with straight-down sedimentation only when viscoelasticity dominates and broadside-on sedimentation only when inertia dominates.
- (9). In viscous fluids inertia will eventually turn long particles broadside-on, no matter how small $\mathbb{R} > 0$ may be. Relatively larger ratios \mathbb{R} of inertial to viscous forces are required to turn long particles stabilized in straight-down orientations by viscoelastic forces.
- (10). The tilt angle appears to be most strongly correlated with the value of the viscoelastic Mach number $M = U/c$ where U is the terminal velocity and c is the shear wave speed measured on the shear wave speed meter. In aqueous polyox solutions, departure from straight-down settling begins at $M = 1$ and only broadside-on configurations occur when $M > 1$. The change of type from straight-down to broadside-on is nearly a step jump at $M = 1$ in aqueous polyacrylamide.
- (11). Spheres falling close to a wall rotate as if rolling down the wall in the intuitive way in a viscous liquid, but rotate as if rolling up the wall against intuition in a viscoelastic liquid. This rolling is anomalous because the angular velocity of the anomalous rolling increases with the fall speed. The phenomenon correlates with the product $E^{1.31} \mathbb{R}^{1.08}$.

ACKNOWLEDGEMENTS

This paper is dedicated to the memory of Joe Matta.

Our work was supported by the NSF, fluid, particulate and hydraulic systems, by the US Army, Mathematics and AHPCRC, and by the DOE, Department of Basic Energy Sciences. We wish to thank R. Bai for his help with experiments and video tape recording, G. Ribeiro for suggesting that we plot the tilt angle against $\Re W_\alpha$ and for other comments, and J. Zhang, H. Vinagre, T. Blomstrom and M. Arney who measured the rod climbing constants, surface tensions, shear wave speeds and viscosities.

REFERENCES

- Allen, E and Uhlherr, P.H.T. 1989 Nonhomogeneous sedimentation in viscoelastic fluids. *J. Rheology* **33**, 627-638.
- Ambari, A., Deslouis, C. and Tribollet, B. 1984 Coil-stretch transition of macromolecules in laminar flow around a small cylinder. *Chem. Eng. Commun.* **29**, 63-78.
- Beavers, G.S. and Joseph, D.D. 1975 The rotating rod viscometer. *J. Fluid Mech.* **69**, 475-511.
- Crochet, M.J. and Delvaux, V. 1990 Numerical simulation of inertial viscoelastic flow, with change of type, in *Nonlinear Evolution Equations that Change Type*(eds. B. Keyfitz and M. Shearer). Springer-Verlag, New York.
- Fraenkel, L.E. 1988 Some results for a linear, partly hyperbolic model of viscoelastic flow past a plate, in *Material Instabilities in Continuum Mechanics and Related Mathematical Problems*(ed. J.M. Ball). Clarendon Press, Oxford.
- Fraenkel, L.E. 1991 Examples of supercritical, linearized, viscoelastic flow past a plate. *J. Non-Newtonian Fluid Mech.* **38**, 137-157.
- Hermes, R.A. and Fredrickson, A.G. 1967 Flow of viscoelastic fluids past a flat plate. *AIChE J.* **13**, 253-259.
- Highgate, D.J. 1966 Particle migration in cone-plate viscometry of suspensions. *Nature*, **211**, 1390-1391; D.J. Highgate and R. W. Whorlow (Ed.), *Polymer Systems: Deformation and Flow*, Macmillan, London, 1968, 251-261.
- Highgate, D.J. and Whorlow, R. W. 1969 End effects and particle migration effects in concentric cylinder rheometry. *Rheol. Acta*, **8**, 142-151.
- Hu, H.H. and Joseph, D.D. 1990 Numerical simulation of viscoelastic flow past a cylinder. *J. Non-Newtonian Fluid Mech.* **34**, 347-377.
- Hu, H.H. and Joseph, D.D. and Fortes, A.F. 1992 Experiments and direct simulations of fluid particle motions. To appear in *Int. Video J. of Eng. Research* **3**.
- James, D.F. 1967 Laminar flow of dilute polymer solutions around circular cylinders, Ph.D. Thesis. Cal. Inst. Tech. Pasadena.

- James, D.F. and Acosta, A.J. 1970 The laminar flow of dilute polymer solutions around circular cylinders. *J. Fluid Mech.* **42**, 269-288.
- Joseph, D.D. 1985 Hyperbolic phenomena in the flow of viscoelastic fluids, in *Viscoelasticity and Rheology* (eds. A.S. Lodge, J. Nohel, and M. Renardy). Academic Press.
- Joseph, D.D. 1990 *Fluid Dynamics of Viscoelastic Liquids*, Springer-Verlag, New York.
- Joseph, D.D. 1992 Bernoulli equation and the competition of elastic and inertial pressures in the potential flow of a second order fluid. *J. of Non-Newtonian Fluid Mech.*, to appear, **42**.
- Joseph, D.D., Arney, M.S., Gillberg, G., Hu, H., Hultman, D., Verdier, C. and Vinagre, T. M. 1992 A spinning drop tensioextensometer. *J. Rheology* **36**, 621-662.
- Joseph, D.D., Matta, J. and Chen, K. 1987 Delayed die swell. *J. Non-Newtonian Fluid Mech.* **24**, 31-65.
- Joseph, D.D., Narain, A. and Riccius, O. 1986 Shear-wave speeds and elastic moduli for different liquids. Part 1: Theory. *J. Fluid Mech.* **171**, 289-308.
- Joseph, D.D., Nelson, J., Hu, H.H. and Liu, Y.J. 1992 Competition between inertial pressures and normal stresses in the flow induced anisotropy of solid particles. To appear at XIth Int. Congress on Rheology, Brussels, Belgium, August 17-21.
- Joseph, D.D., Riccius, O. and Arney, M.S. 1986 Shear-wave speeds and elastic moduli for different liquids. Part 2: Experiments. *J. Fluid Mech.* **171**, 309-338.
- Leal, L.G. 1975 The slow motion of slender rod-like particles in a second-order fluid. *J. Fluid Mech.* **69**, 305-337.
- Michele, J. Pätzold, and R. Donis, R. 1977 Alignment and aggregation effects in suspensions of sphere in non-Newtonian media. *Rheol. Acta*, **16**, 317-321.
- Petit, L. and Noetinger, B. 1988 Shear-induced structure in macroscopic dispersions. *Rheol. Acta*, **27**, 437-441.
- Thompson, W. and Tait, P.G. 1879 *Natural Philosophy*, 2nd Ed., Cambridge.
- Ultman, J.S. and Denn, M.M. 1970 Anomalous heat transfer and a wave phenomenon in dilute polymer solutions. *Trans. Soc. Rheol.* **14**, 307-317.

List of Figures

Figure 1.....	4
---------------	---

Figure 1. Potential flow past a cylinder. The pressure at stagnation points s will turn the broadside of the body into stream. If the extensional stress at s were reversed, as may be

possible in a viscoelastic liquid, the body would line up with the stream. The same effect could be provided by normal stresses caused by strong shears at the corners c . In practice, viscosity will lead to boundary layers and wakes whose effects are not yet understood.

Figure 2.....9

Figure 2. Measured zero shear rate viscosities η (cps) of aqueous solutions of polyox (Union Carbide, Products Manual [1981]). (a) solution viscosity at 25°C vs. percentage of polyox in water by weight. This curve was fitted to the formula

$$\eta = \{\text{Error!}\}$$

where p is percentage of polyox. (b) solution viscosity for 1% polyox vs. temperature T (°C), $\eta = 4532 e^{-0.028037T}$.

Figure 3.....10

Figure 3. Climbing constants of aqueous solutions of polyox. (a) climbing constant vs. percentage of polyox in water at $T=24^\circ\text{C}$; (b). climbing constant of 1% polyox in water vs. temperature.

Figure 4.....10

Figure 4. Surface tensions σ (dyne/cm) of aqueous solutions of polyox WSR-301 vs. percentage of polyox in water at room temperature.

Figure 5.....11

Figure 5. Shear wave speed c in aqueous solutions of polyox vs. percentage of polyox in water at room temperature.

Figure 6.....15

Figure 6. Schematic diagram of the experimental set-up.

Figure 7.....16-18

Figure 7 The effect of the concentration of polyox in water on the tilt angle ($T=24^\circ\text{C}$). (a) teflon, (b) titanium, (c) tin, (d) brass cylinders. When $\theta=0^\circ$ the motion is dominated by inertia; when $\theta=90^\circ$ the motion is dominated by normal stresses. As the concentration increases the tilt angle θ becomes larger. Figure 7(e) shows titanium cylinders with $(D,L)=(0.25,0.8)$ in. falling in the aqueous solutions of polyox of various concentrations. \circ $L=0.4$ in., \square $L=0.6$ in., \diamond $L=0.8$ in., $+$ $L=1$ in. for flat ends, \bullet $L=0.8$ in. (round ends), \blacktriangle $L=0.8$ in. (cone ends).

Figure 8.....19-21

Figure 8 The effect of cylinder weight on the tilt angle ($T=24^\circ\text{C}$). (a) cylinders with same length $L=0.4$ in. but different densities falling in 0.75% polyox/water solution, (b)

cylinders with $L=0.6$ in. in 0.85% polyox/water solution, (c) cylinders with $L=1.0$ in. in 1.0% polyox/water solution, (d) cylinders with $L=0.4$ in. in 1.5% polyox/water solution. The heavier the cylinder, the smaller the tilt angle. The pictures in Figure 8(e) show how cylinders with $L=0.8$ in. fall in 0.85% polyox/water solution.

Figure 9.....22-23

Figure 9. The effect of cylinder length on the tilt angle ($T=24^{\circ}\text{C}$). (a) aluminum cylinders in 1.0% polyox/water solution, (b) brass in 1.5% solution, (c) titanium in 1.25% solution, (d) stainless steel in 1.0% solution, (e) aluminum in 0.75% solution, (f) teflon in 0.6% solution.

Figure 10.....23-24

Figure 10. The effect of cylinder shape on the tilt angle ($T=24^{\circ}\text{C}$). (a) cylinders with same length $L=0.8$ in. but with flat ends, round ends and cone ends respectively, falling in 1.0% polyox/water solution, (b) the same cylinders falling in 1.25% solution, (c) and (d) brass cylinders falling in 1.0% and 1.5% solutions. \circ flat ends, \bullet round ends, \blacktriangle cone ends.

Figure 11.....25

Figure 11. The effect of liquid temperature on the tilt angle. (a) tin cylinders falling in 1.0% polyox/water solution at different temperatures, (b) a brass cylinder with $(D, L)=(0.25, 1.0)$ in. in 1.0% polyox/water solution at different temperatures. As the temperature increases, the tilt angle decreases.

Figure 12.....29

Figure 12. Tilt angle θ vs. Reynolds number (a) and tilt angle vs. Mach number (b) for cylinders with $L=0.8$ in. in polyox/water solutions of various concentrations. \square flat ends, \bullet round ends, \blacktriangle cone ends.

Figure 13.....30

Figure 13. Tilt angle θ vs. Reynolds number (a) and tilt angle vs. Mach number (b) for all the data, cylinders of all lengths, shapes and weights in polyox/water solutions: \triangle 1.5%, \circ 1.25%, \diamond 1%, \times 0.85%, $+$ 0.75%, \blacklozenge 0.6%, \bullet 0.5%.

Figure 14.....31

Figure 14. Tilt angle θ vs. Reynolds number (a) and tilt angle vs. Mach number (b) for cylinders with $L=0.8$ in. (most with round ends) in 2% aqueous polyacrylamide, \triangle $D=0.1$ in., \times $D=0.15$ in., \bullet $D=0.25$ in., \circ $D=0.25$ in. (flat ends), \diamond $D=0.35$ in., \blacklozenge $D=0.4$ in.

Figure 15.....35-36

Figure 15. Anomalous rolling of a sphere on a wall inclined from the vertical in polyox/water solutions: (a) angular speed ω vs. the angle of inclination from horizontal

(90° is vertical). (b) ω vs. R . (c) measured ω vs. calculated ones from the correlation (7.5). ○ 1% polyox, flat surface; △ 1.25% polyox, flat surface; ▲ 1.25% polyox, wire surface; □ 1.5% polyox, flat surface; ■ 1.5% polyox, wire surface.

List of Tables

Table1.....11
 Table 1. Physical properties of polyox WSR-301/water solutions

Table2.....13-14
 Table 2. Test particles

Table3.....27-28

Table 3. Tilt angle response of sedimenting cylinders in 2% aqueous polyacrylamide (Cyanamer N-300 LMW) at room temperature. The zero shear viscosity is $\eta = 9$ poise. The molecular weight is about 5×10^6 . The value of the shear-wave speed measured on the wave speed meter is $c = 16.72$ cm/sec. The surface tension and climbing constant are $\sigma = 45$ dyne/cm and $\hat{\beta} = 96.4$ g/cm respectively.

CONTENTS OF APPENDIXES

A. Summary of the experimental data.....46
 Nomenclature in the tables.....46
 A1. Sedimentation in aqueous polyox with different concentrations (T=24°C).....46
 A1.1. 1.5% aqueous polyox.....46
 A1.2. 1.25% aqueous polyox.....48
 A1.3. 1.0% aqueous polyox.....49
 A1.4. 0.85% aqueous polyox.....50
 A1.5. 0.75% aqueous polyox.....52
 A1.6. 0.6% aqueous polyox.....53
 A1.7. 0.5% aqueous polyox.....54
 A2. Sedimentation in 1.0% aqueous polyox at different temperatures.....54
 A2.1. T=23.5°C.....54
 A2.2. T=34°C.....55
 A2.3. T=45°C.....56
 A2.4. T=58.5°C.....57
 A3. Sedimentation in 2% aqueous polyacrylamide (T=24°C).....58
 A4. Sphere falling close to a wall in aqueous polyox

at room temperature.....	60
A4.1. 1.5% aqueous polyox.....	60
A4.2. 1.25% aqueous polyox.....	60
A4.3. 1.0% aqueous polyox.....	61
B. Plots of experimental results.....	62
Nomenclature in the plots.....	62
B1. Sedimentation in aqueous polyox with different concentrations (T=24°C).....	62
B1.1. 1.5% aqueous polyox.....	62
B1.2. 1.25% aqueous polyox.....	64
B1.3. 1.0% aqueous polyox.....	66
B1.4. 0.85% aqueous polyox.....	68
B1.5. 0.75% aqueous polyox.....	70
B1.6. 0.6% aqueous polyox.....	72
B1.7. Tilt angle vs. concentration.....	73
B2. Sedimentation in 1.0% aqueous polyox at different temperatures.....	74
C. Correlations of tilt angle vs. Reynolds number \mathbb{R} and Mach number M.....	75
C1. Tilt angle vs. \mathbb{R} for different concentrations.....	75
C2. Tilt angle vs. \mathbb{R} for different lengths of cylinders.....	76
C3. Tilt angle vs. M for different concentrations.....	77
C4. Tilt angle vs. M for different lengths of cylinders.....	78